DTU Library

Techno-economic analysis on the integration of an electrified clay calcination process into a cement plant

Laurini, Bruno; Zong, Yi; Træholt, Chresten; Parra, Sebastian Andres Quevedo; Shanmugasundaram, Meenakshisundaram

[Link back to DTU Orbit]()

Techno-economic analysis on the integration of an electrified clay calcination process into a cement plant

Bruno Laurini[1*], Yi Zong[1], Chresten Træholt[1], Sebastian Andres Quevedo Parra[2], Meenakshisundaram Shanmugasundaram[3]

1 Department of Wind and Energy Systems, Technical University of Denmark, 2800 Kgs. Lyngby, Denmark

2 Department of Energy, Politecnico di Milano, Milan, Italy

3 FLSmidth Private Limited, Chennai, India

(*Corresponding Author: brulau@dtu.dk)

ABSTRACT

Calcined clay, as supplementary cementitious material (SCM), can potentially reduce the cement industry's carbon footprint by partly avoiding CO_2 emissions released from clinker production. Further reduction can be achieved through the electrification of the clay calcination process while coupled with increasing penetration of renewable energy sources (RES). This paper addresses the economic and CO_2 emissions performance of an electrified clay calcination process integrated into a reference cement plant. An optimal sizing algorithm is developed to investigate how local renewable-based generation and high-temperature thermal storage can be exploited to improve the economic feasibility of electrification. Results show that even without optimization, the integration allows a reduction of the overall cost of cement for a given geographic area and considering a carbon price of 100 €/tCO2. When applying the optimal sizing algorithm, an additional decrease in costs is observed, primarily due to the lower energy costs achieved by installing a 41.18 MW PV plant and a 340 MWh thermal storage.

Keywords: calcined clay, cement, techno-economic analysis, optimal sizing, electrification, renewable generation

NONMENCLATURE

Abbreviations	
CAC	Cost of CO2 avoided
CAPEX	Capital expenditures
COC	Cost of clinker/cement
EHGG	Electric hot gas generator

ELCC	Integration of electrified clay calcination option
ELCC-RES	Integration of electrified clay calcination option
NPV	Net present value
OPEX	Operational expenditures
REF	Reference cement plant option
SCM	Supplementary cementitious material
TES	Thermal energy storage

1. INTRODUCTION

The cement industry currently accounts for approximately 7% of the world's carbon dioxide emissions and is the third largest industrial energy consumer [1]. One of the main factors that contribute to this large share of emissions is the high clinker-to-cement ratio of conventional cement blends. This is due to the production of clinker, which involves the combustion of fossil fuels and thermal decomposition (calcination) of limestone. In fact, around 60-65% of the carbon dioxide emissions related to cement production comes from the calcination process and 35-40% originates from the combustion of fossil fuels in cement ovens (i.e., kilns) [2].

One solution to help decarbonize the cement sector is to partially substitute clinker with Supplementary Cementitious Materials (SCMs), such as calcined clay. For instance, Limestone Calcined Clay Cement (LC3) is a relatively new cement type made by blending clinker with calcined clay, limestone, and gypsum. Such blend has the potential to reduce the CO_2 emissions associated with cement manufacturing by 15–30% [3]. To further reduce emissions, the thermal energy needed to calcine the clay could be delivered by cleaner energy vectors, e.g., biofuels, green hydrogen, and electricity [4]. In the

case of using electricity, a Power-to-Heat (P2H) approach is exploited, where different methods can be used to convert electricity into thermal energy (e.g., plasma heating, microwave heating, and resistive electrical heating) [5].

To promote the adoption of carbon mitigation technologies in the cement industry, conducting techno-economic assessments is crucial. These assessments offer valuable insights into the economic performance of such technologies and allow for meaningful evaluations alongside benchmark solutions. For example, inside the CEMCAP project, studies have been carried out to develop an economic model that facilitates the comparison between different CO_2 capture technologies, including MEA-based absorption, oxyfuel, and calcium looping, among others [6,7]. The model relies on economic parameters such as CAPEX and OPEX values, as well as results from process simulations for each plant layout configuration [8]. In these studies, the outputs for different technologies were then compared, for instance, with respect to the cost of the clinker produced and cost of avoided CO_2. The last metric allows for an assessment of the cost increase associated with CO_2 abatement.

When considering electrified processes or energy intensive industries, operational costs from energy-related expenses play a significant role in the economic feasibility of a project. In this sense, energy planning tools can support decision-making by providing sizing and investment strategies on energy technologies that are close to the true cost-optimal solution.

A two-stage optimization approach was proposed to optimally size a renewable-based energy system for a food factory in China [9]. In the first stage, all feasible solutions are obtained through The Hybrid Optimization of Multiple Energy Resources (HOMER) software. Then, in the second stage, the Vise Kriterijumska Optimizacija I Kompromisno Resenje (VIKOR) method is used to select the optimal solution based on a multi-criteria evaluation of the feasible solutions taking into account energy, economic, and environmental factors. In another study, an optimal design model is proposed for an industrial microgrid in China, considering PV and batteries [10]. The particle swarm optimization (PSO) method is applied, and case studies show that the optimal installation of batteries has significant impacts over economic and environmental indicators when compared to the baseline scenario. This baseline considers the existing configuration of the microgrid, with only 500 kW of PV installed. Additionally, in [11], a reliability-constrained optimal sizing algorithm was developed to size an energy storage system within a microgrid. This is achieved using a mixed-integer programming model, with the goal of minimizing investment and operating costs while satisfying specific constraints. One of these constraints refers to ensuring a certain level of reliability, specifically by limiting the Loss of Load Expectation (LOLE) to a predefined target value.

This paper presents a techno-economic analysis of integrating an electrified clay calcination process into a cement plant. To highlight the impact of energy supply on economic and emissions performance, the paper also introduces an optimization methodology for sizing a renewable-based energy system, that meets local electrical and heat demands. A Thermal Energy Storage (TES) system is also modelled, so that its potential to enhance the power flexibility of the cement plant under different pricing schemes is investigated. The CEMCAP project and its economic model are used as guidelines for defining cost parameters and providing the characteristics of a reference cement plant, which is used as benchmark for the analysis.

2. METHODOLOGY

The methodology used in the study consists of three main steps. First, the performance of the CEMCAP reference plant is assessed. Second, calculations are made to emulate the integration of an electrified clay calcination process, which uses electricity directly from the power network where the plant is connected to. Finally, the same integration is analyzed but through the development of a Mixed Integer Linear Programming (MILP) optimization model, that optimally sizes on-site renewable generation and energy storage.

2.1 Reference cement plant

The performance of the reference CEMCAP plant is evaluated by two main metrics: the cost of clinker/cement (COC) in $€/t_{cem}$, and the specific equivalent emissions ($e_{cem,eq}$) in t_{co2}/t_{cem}. The COC is calculated as the cost of clinker that would make the net present value (NPV) go to zero in the last year of the project (Y). The NPV is formulated as follows:

$$NPV = \sum_{y=y_{ini}}^{0} \left[-\frac{CAPEX_y}{\left(1 + \frac{r}{100}\right)^y} \right] + \sum_{y=1}^{Y} \left[\frac{rev_y - OPEX_y}{\left(1 + \frac{r}{100}\right)^y} \right] \quad (1)$$

Where y_{ini} is the year in which the plant starts to be constructed, being negative since year one represents the first operational year of the plant. $CAPEX_y$ is the amount of capital investment allocated to year y. $OPEX_y$ and rev_y are the operational costs and the revenues, respectively, associated to year y, and r is the discount rate given in percentage. Since capital costs were given

for 2014 in the CEMCAP framework, the Chemical Engineering Plant Cost Index (CEPCI) is used to update them to the year 2021, which is the year taken as reference for the cost of renewable generators.

2.2 Electrified clay calcination

The electrified calcination process is based on a flash calciner which uses resistive heating technology, i.e., an electric hot gas generator (EHGG), to provide the required thermal energy for calcination. It is sized to match the material demand of calcined clay for producing LC^3-50. This cement blend consists of a mixture of 50% clinker, 30% calcined clay, 15% limestone and 5% gypsum [12].

The integration proposed here considers a brownfield scenario, where the capacity of the reference plant is increased by the introduction of a calcined clay line. Therefore, it is assumed that there is no significant change in the clinker production process and the values of utilities and consumables are maintained the same. However, the new line's implementation yields significant effects:

- Higher cement capacity
- An increase in the total plant cost (TPC) due to the installation of the new line and the EHGG
- An increase in the electricity consumption due to auxiliary equipment of the new line
- A heat demand that needs to be supplied by the EHGG

As expected, these changes impact the COC and the emissions associated with the plant. Here, it is important to differentiate between scope 1 and scope 2 carbon emissions. The first scope regards direct emissions that occur inside of the plant, e.g., from the burning of fossil fuels in one of the plant's processes, whilst the second scope comes from indirect emissions, e.g., from the generation of the energy that is being purchased by the plant. The overall CO_2 emissions are quantified by summing the contribution of the clinker production (e_{clk}) and the indirect emissions associated to purchasing electricity ($e_{el,cem}$):

$$e_{cem,eq} = \frac{e_{clk} m_{clk}}{m_{cem}} + e_{el,cem} \qquad (2)$$

Where m_{clk} and m_{cem} are the yearly production of clinker and cement in metric tons. The indirect emissions are calculated based on the grid emission factor of the specific location where the plant is situated. Another important key performance indicator (KPI) is the cost of CO_2 avoided (CAC), expressed in €/t$_{CO2}$. The CAC reflects the cost associated with reducing carbon dioxide emissions and is a widely used metric for evaluating the performance of carbon capture technologies.

$$CAC = \frac{COC - COC_{ref}}{e_{cem,eq,ref} - e_{cem,eq}} \qquad (3)$$

2.3 MILP model

The optimization algorithm is applied only to the energy supply part of the cement plant, considering the active power balance of the whole plant and thermal power balance of the clay calcination process. Thermal power flows of the clinker production process are not analyzed here since they are already considered in terms of fuel consumption of the reference plant. Two types of renewable generators (i.e., PV modules and Wind turbines) and two types of thermal technologies (i.e., TES and EHGG) are modeled. Moreover, the model is based on a yearly time horizon (8760 hours) with a timestep of one hour. The model is developed in a Julia/JuMP environment using Gurobi as a solver.

2.3.1 PV plant

The PVGIS tool [13] is employed to estimate global (G_t^H) and diffuse ($G_t^{H,diff}$) values of horizontal irradiance considering typical meteorological year (TMY) data. Solar angles are calculated based on geographic information and PV module's orientation, which includes surface tilt and azimuth. This calculation allows for the estimation of hourly values of global irradiance on a tilted surface (G_t^T) [14]. In this analysis, a fixed-tilt PV system is considered.

$$G_t^T = G_t^H \left(1 - \frac{G_t^{H,diff}}{G_t^H}\right) Rb_t + G_t^{H,diff} \left(\frac{1+cos(\beta^{PV})}{2}\right) + G_t^H \rho \left(\frac{1-cos(\beta^{PV})}{2}\right) \qquad (4)$$

Where Rb_t is the ratio of beam radiation on tilted surface, β^{PV} is the tilt angle of the module and ρ is the albedo, which is here defined as 0.2. The power generated by a single module ($P_t^{PV,uni}$) can be calculated as follows:

$$P_t^{PV,uni} = \eta^{PV,ref}\left[1 - \mu\left(T_t^{cell} - T^{cell,STC}\right)\right]G_t^T A^{PV} \qquad (5)$$

Where $\eta^{PV,ref}$ is the module's efficiency at standard test conditions (STC), μ is the temperature coefficient, T_t^{cell} is the temperature of the cell, $T^{cell,STC}$ is the temperature of the cell at STC, and A^{PV} is the surface area of one module. To address variations in module efficiency caused by temperature changes, T_t^{cell} is estimated based on the dry-bulb air temperature ($T_t^{a,DB}$), which is available in the PVGIS TMY dataset, the nominal operating cell temperature of the module ($T^{cell,NOCT}$), and solar irradiance on the tilted surface.

$$T_t^{cell} = T_t^{a,DB} + (T^{cell,NOCT} - 20)\frac{G_t^T}{800} \qquad (6)$$

The overall power produced by the PV plant (P_t^{PV}) is calculated by multiplying $P_t^{PV,uni}$ by the number of modules (N^{PV}), which is a decision variable, and the balance of the system efficiency (η^{BOS}).

2.3.2 Wind turbines

Hourly wind speed data for 2021 were collected from NASA's POWER project [15]. Wind speed measurements at different heights are used to estimate an average power law coefficient, and then extrapolate the wind speeds to the desired hub height of the wind turbine.

Discrete power curve values are used to fit a spline, so that the power can be obtained according to any wind speed inside the operating region of the turbine. Furthermore, the number of wind turbines is a decision variable that multiplies the power produced by a single turbine, so that the overall wind power can be estimated.

2.3.3 TES and EHGG

Both the TES and EHGG considered here are technologies that can convert electrical power to high temperature thermal power through resistive heating. The main difference is that the TES utilizes solid material with high thermal capacitance to store heat, whereas the EHGG dissipates heat directly to the gas stream, without an energy buffer.

The hot gas generator simply converts electrical ($P_t^{el,EHGG}$) power to thermal power ($P_t^{th,EHGG}$) based on its rated efficiency (η^{EHGG}). Its rated maximum power is a decision variable ($P_t^{el,EHGG,max}$), which is directly linked to its capital cost.

$$P_t^{th,EHGG} = \eta^{EHGG} P_t^{el,EHGG} \qquad (7)$$

Conversely, the thermal storage model is based on an intertemporal constraint that links two subsequent time periods:

$$E_{t+1}^{th,TES} = E_t^{th,TES} + \left(P_t^{el,TES,ch} \eta^{TES,ch} - \frac{P_t^{th,TES,dch}}{\eta^{TES,dch}} \right) \Delta t \qquad (8)$$

Where $E_t^{th,TES}$ is the thermal energy stored at time t. $P_t^{el,TES,ch}$ and $P_t^{th,TES,dch}$ are the charging and discharging powers. $\eta^{TES,ch}$ and $\eta^{TES,dch}$ are the charging and discharging efficiencies. It is assumed that the unitary storage can be stacked in a modular way to increase energy capacity and maximum charging/discharging rates.

2.3.4 Power balances

Two types of power balances are defined while assuming a single node model, i.e., power flows are injected and absorbed into/from the same node. First, the active power balance is defined as:

$$P_t^{PV} + P_t^{WT} + P_t^{grid,abs} = D_t^{el} + P_t^{EHGG,el} + P_t^{el,TES,ch} + P_t^{grid,inj} \qquad (9)$$

Where $P_t^{grid,abs}$ is the power absorbed from the grid, D_t^{el} is the electrical demand of the cement plant, and $P_t^{grid,inj}$ is the power injected into the grid. It is worth mentioning that binary decision variables ($x_t^{grid,inj}$ and $x_t^{grid,abs}$) are introduced to prevent simultaneous injection and absorption of power into/from the grid. Eqs. 10-12 enforce the non-simultaneity constraint.

$$x_t^{grid,inj} + x_t^{grid,abs} \leq 1 \qquad (10)$$
$$P_t^{grid,inj} \leq P_t^{grid,inj,max} x_t^{grid,inj} \qquad (11)$$
$$P_t^{grid,abs} \leq P_t^{grid,abs,max} x_t^{grid,abs} \qquad (12)$$

The thermal power balance is set considering only the clay calcination process.

$$P_t^{EHGG,th} + P_t^{th,TES,dch} = D_t^{th} \qquad (13)$$

2.3.5 Objective function

The objective function to be maximized is represented by Eq. 1. Where new cost values are added along with those related to the reference plant. For instance, the CAPEX now includes investment costs related to renewable generators and thermal technologies. Likewise, OPEX now includes O&M costs of installed technologies, but also operational expenses related to buying power from the grid. In theory, surplus power can also be sold and generate revenue.

3. RESULTS AND DISCUSSION

The analysis performed based on the aforementioned methodology consists in comparing KPIs of the three different options:

- Reference cement plant (REF)
- Integration of electrified clay calcination with the cement plant not considering optimal sizing of on-site generation and energy storage (ELCC)
- Integration of electrified clay calcination with the cement plant considering optimal sizing of on-site generation and energy storage (ELCC-RES)

The performance of such layouts is location dependent, especially for ELCC and ELCC-RES, mainly due to the dependency on local costs of technologies, electricity prices, grid emission factor and RES potential. Therefore, a site in France is defined for the analysis.

3.1 Input data

The main inputs regarding the operation of the cement plant considered for the three cases are presented in Table 1. The parameters related to the clinker production process used in the CEMCAP economic model are the same for all the configurations,

since the clinker output is maintained while increasing the overall cement throughput, when calcined clay is used as a SCM.

Table 1 - Main operational parameters of the cement plant

Parameter	REF	ELCC/ELCC-RES
Clinker production	2895.5 t_{clk}/day	2895.5 t_{clk}/day
Capacity factor	91.3%	91.3%
Clinker-to-cement ratio	0.735	0.5
Calcined clay production	-	1737.3 t_{cc}/day
Raw meal	1.66 $t_{RawMeal}$/t_{clk}	1.66 $t_{RawMeal}$/t_{clk}
Fuel	3.135 GJ_{LHV}/t_{clk}	3.135 GJ_{LHV}/t_{clk}
Electricity (only for clinker)	131.9 kWh_{el}/t_{clk}	131.9 kWh_{el}/t_{clk}
Electricity (clay calcination)	-	7.9 kWh_{el}/t_{cc}
Heat (clay calcination)	-	455.5 kWh_{th}/t_{cc}
Amonia solution	5 kg_{NH3}/t_{clk}	5 kg_{NH3}/t_{clk}

The cost of the technologies included in the MILP model is shown in Table 2. The PV system is considered to be south-oriented, with a tilt of 15°, and with a balance of the system of 87%. The grid emission factor is set as 58 gCO_2e/kWh [18], to account for the indirect carbon dioxide emissions when power is bought from the grid. Such value is low compared to other countries due to the high share of nuclear energy in France's electricity mix. An average industrial price of electricity of 111.5 €/MWh is used as reference [19]. To investigate the impact of dynamic pricing schemes on the solution, data from the day-ahead (DA) market in France with respect to 2021 is used [20]. The dynamic behavior of the DA prices through the year is averaged to represent a single day, then the hourly values are scaled to have a mean of 111.5 €/MWh. In such a way, the comparison between uniform and dynamic pricing is more realistic. Moreover, no selling price or incentive for injecting surplus power into the grid is set in the case study.

Table 2 - Cost of technologies [16,17] and technical parameters

Technology	CAPEX	OPEX	Rated capacity	Efficiency
PV	743.5 €/kW	14.1 €/kW	400 W	20.77 %
Wind turbines	1504.7 €/kW	45 €/kW	2 MW	-
EHGG	60 €/kW	-	-	95 %
TES	50 €/kWh	0.4 €/kWh	340 MWh	98 %

The installation of photovoltaic modules and wind turbines is subjected to a land-related constraint, where the maximum available area for use is set as 1.25 km2. The land requirements for PV and wind turbines are assumed to be approximately 7.5 acres/MW and 85.25 acres/MW, respectively [21] [22].

3.2 Comparison of results

The main results related to the performance of the three options are shown in Table 3. No carbon price is assumed at this stage. It is noted that the cost of cement for the scenarios with electrification is higher than the reference one. However, the ELCC-RES show relatively lower COC than the ELCC, mainly due to the lower electricity OPEX, which consequently reduces the annual expenses of the plant. Even if the difference of COC for these two cases is not large, there is a significant difference with respect to their CAC, reaching close to 16 €/t_{CO2}.

Table 3 - Main results for the three options

Option	COC [€/t_{cem}]	CAC [€/t_{CO2}]	TPC [M€]	Expenses [M€]	Electricity OPEX [M€]
REF	56.74	-	250.69	50.06	14.65
ELCC	66.74	51.99	387.60	91.07	47.12
ELCC-RES	63.55	35.13	434.22	80.37	35.71

A lower value of CAC for the ELCC-RES scenario means that a lower carbon price is needed to make its COC equal to the reference one. Furthermore, it is interesting to note that even though the TPC increases substantially in the ELCC-RES case, due to the installation of PV and storage, the positive effect of the lower electricity OPEX over the COC is more significant.

The cost breakdown of cement for the different cases can be seen in Figure 1. It is noted that CAPEX and fixed costs represent the main contributions in the REF scenario. Instead, ELCC reveals a larger contribution of electricity costs, which is approximately twice as much as in the reference case. As previously mentioned, ELLC-RES is characterized by lower electricity costs at the expense of having a higher CAPEX contribution, when compared to ELCC. Also, it is noted that the impact of fuel and raw material into the COC slightly decreases due to partial electrification and reduction of clinker-to-cement ratio.
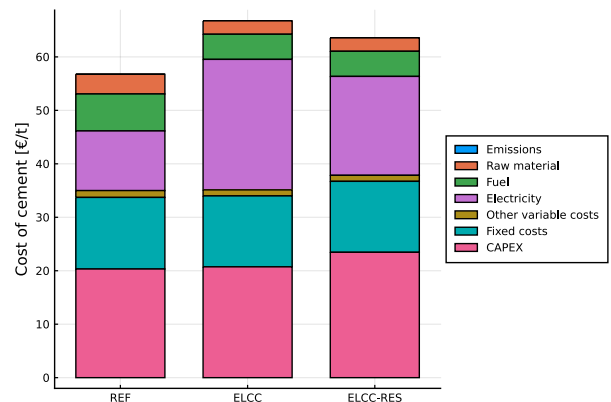

Figure 1 - Cost breakdown of cement

Table 4 shows the installed technologies in the ELCC-RES case. In terms of on-site generation, 41.18 MW of PV are installed while the wind capacity is 0 MW. This
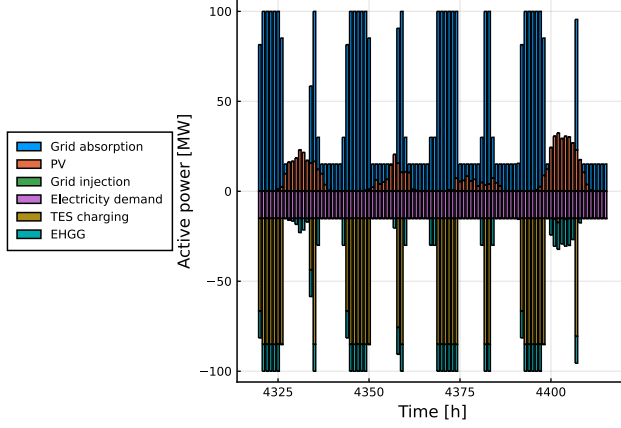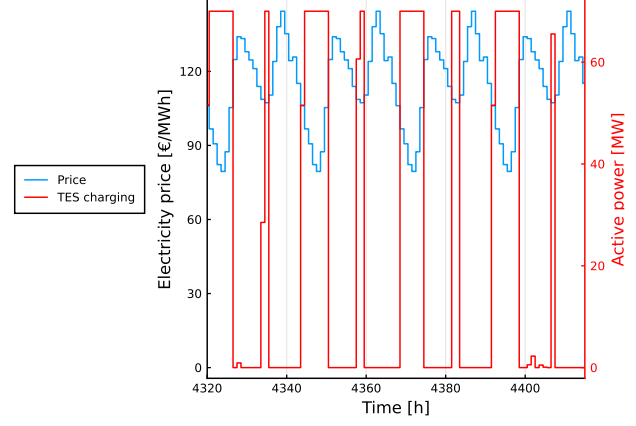
Figure 2a - Active power balance

Figure 2b - TES charging strategy according to electricity price

Figure 2 - Power dispatch during four consecutive summer days

probably occurs due to the combined effect of lower land requirement and lower CAPEX of PV with respect to wind turbines, even though the capacity factor of the latter is almost three times higher. Another interesting point is the selection of TES for supplying the heating demand in conjunction with a smaller EHGG. However, it is important to point out that the TES is selected only when the dynamic pricing scheme is set, since the storage can allow charging in hours of low electricity price. In fact, it is noted that the energy arbitrage provided by the TES accounts for a reduction of almost 5 M€ in the electricity OPEX. This is analyzed by forcing the model to not choose storage and comparing the annual expenses.

Table 4 - Installed technologies in ELCC-RES case

Technology	Installed capacity	Capacity factor	CAPEX
PV	41.18 MW	12.87 %	30.62 M€
Wind turbines	0 MW	36.02 %	0 M€
EHGG	14.95 MW	-	0.9 M€
TES	340 MWh	-	17 M€

Figure 2 shows the active power balance and the charging profile of the storage during four subsequent summer days. It is noted that the power produced by the PV plant only supplies part of the demand, which is characterized by three different contributions: the electricity demand of the whole plant, the power used to supply the EHGG and the TES charging power. The thermal storage improves the economic performance by increasing flexibility and charging when electricity is cheaper, i.e., during the first hours of the day. The EHGG is used as an auxiliary asset, to top up the thermal power needs and allow the storage to achieve the most optimal utilization of its capacity.

In terms of emissions, REF, ELCC and ELCC-RES are defined by approximately 0.627 t_{co2}/t_{cem}, 0.435 t_{co2}/t_{cem} and 0.433 t_{co2}/t_{cem}, respectively. The quite small change observed in the two last cases are most likely linked to:

- Higher contribution of direct emissions (coming from clinker production) on the overall emissions

- Very low grid emission factor in France

- Not large contribution of local renewable generation over the total electricity supply

Therefore, it is noted that the benefits related to installing on-site renewable generation and thermal storage are primarily centered around the economic aspect rather than the environmental one. However, the difference in emissions from these two options can become more evident when increasing land availability and considering countries that have a high share of fossil fuel power plants in their electricity generation mix.

3.3 Effect of carbon price

Carbon pricing has a direct influence on the COC since the cost of emissions can be included in the OPEX term of Eq. 1. As an example, when considering a carbon price of 100 €/t_{co2}, which can be a realistic price within the European Union, the recalculated COC values are as follows: 119.48 €/t_{cem} for REF, 110.25 €/t_{cem} for ELCC and 106.90 €/t_{cem} for ELCC-RES. Figure 3 shows the new cost breakdown for the three cases. In this context, it becomes evident that the electrified options outperform the reference one due to their lower specific emissions. It is worth noting that the increase in carbon price does not affect the solution in terms of installed technologies of ELCC-RES. This is because the constraint of land availability has already been reached when the carbon price is at zero.
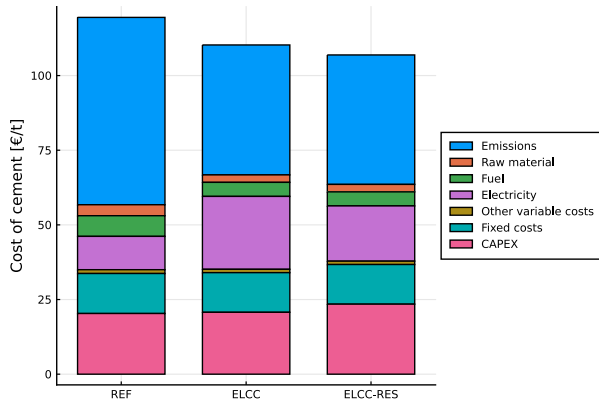
6

Figure 3 - Cost breakdown of cement considering a carbon price of 100 €/t_{co2}

4. CONCLUSIONS

The integration of an electrified clay calcination process with a cement plant is investigated through the assessment of its economic and carbon emissions performance. An optimal sizing algorithm is developed to size on-site renewable generation and a thermal storage system so that electrical and thermal demands can be satisfied while maximizing the net present value of the project. The model chooses to install a PV plant and a thermal energy storage that runs in parallel with an electric hot gas generator. The option that considers optimal sizing (ELCC-RES) performs slightly better both in terms of cost and CO_2 emissions, with respect to the one without it (ELCC). Altogether, both ELCC and ELCC-RES options show lower cost of cement, compared to the reference case, when a carbon price of 100 €/t$_{co2}$ is considered for calculating the cost of emissions. More specifically, the cost of CO_2 avoided for ELCC and ELCC-RES are 51.99 €/t$_{co2}$ and 35.13 €/t$_{co2}$, respectively. Future studies should be performed to explore the extent to which the outcomes depend on the geographic location of the plant. Real-time grid carbon intensity could also play a role in quantifying more accurately scope two emissions savings. Moreover, a sensitivity analysis should also be applied to the capital costs of the plant to deal with price uncertainties and understand how CAPEX variations influence COC and CAC values.

DECLARATION OF INTEREST STATEMENT

The authors declare that they have no known competing financial interests or personal relationships that could have appeared to influence the work reported in this paper. All authors read and approved the final manuscript.

REFERENCE

[1] IEA (2018). Low‑Carbon Transition in the Cement Industry. IEA.

[2] Karlsson, I., Toktarova, A., Rootzén, J., Odenberger, M. Technical Roadmap Cement Industry; Mistra Carbon Exit: Stockholm, Sweden, 2020.

[3] Jaskulski, Roman & Jóźwiak‑Niedźwiedzka, Daria & Yakymechko, Yaroslav. (2020). Calcined Clay as Supplementary Cementitious Material. Materials. 13.

[4] IEA (2022). Cement, IEA, Paris https://www.iea.org/reports/cement, License: CC BY 4.0.

[5] Madeddu, S., Ueckerdt, F., Pehl, M., Peterseim, J., Lord, M., Kumar, K.A., Krüger, C., Luderer, G. (2020). The CO2 reduction potential for the European industry via direct electrification of heat supply (power‑to‑heat). Environmental Research Letters. 15.

[6] Gardarsdottir, S. O., De Lena, E., Romano, M., Roussanaly, S., Voldsund, M., Berstad, D., Fu, C., Anantharaman, R., Sutter, D., Gazzani, M., Mazzotti, M., & Cinti, G. (2018). Comparison of Technologies for CO2 Capture from Cement Production—Part 2: Cost Analysis. Energies, 12(3), 542. https://doi.org/10.3390/en12030542.

[7] De Lena, E.; Spinelli, M.; Romano, M.; Gardarsdottir, S.O.; Roussanaly, S.; Voldsund, M. CEMCAP Economic Model Spreadsheet. 2018. Available online: https://zenodo.org/record/1446522 (accessed on 28 July 2023).

[8] Voldsund, M., Gardarsdottir, S. O., De Lena, E., Jamali, A., Berstad, D., Fu, C., Romano, M., Roussanaly, S., Anantharaman, R., Hoppe, H., Sutter, D., Mazzotti, M., Gazzani, M., Cinti, G., & Jordal, K. (2018). Comparison of Technologies for CO2 Capture from Cement Production—Part 1: Technical Evaluation. Energies, 12(3), 559. https://doi.org/10.3390/en12030559.

[9] Li, X., Gao, J., You, S., Zheng, Y., Zhang, Y., Du, Q., Xie, M., & Qin, Y. (2022). Optimal design and techno-economic analysis of renewable-based multi-carrier energy systems for industries: A case study of a food factory in China. Energy, 244, 123174. https://doi.org/10.1016/j.energy.2022.123174.

[10] M. Mao, P. Jin, L. Chang and H. Xu, "Economic Analysis and Optimal Design on Microgrids With SS-PVs for Industries," in *IEEE Transactions on Sustainable Energy*, vol. 5, no. 4, pp. 1328-1336, Oct. 2014, https://doi.org/10.1109/TSTE.2014.2327067.

[11] S. Bahramirad, W. Reder and A. Khodaei, "Reliability-Constrained Optimal Sizing of Energy Storage System in a Microgrid," in *IEEE Transactions on Smart Grid*, vol. 3, no. 4, pp. 2056-2062, Dec. 2012, https://doi.org/10.1109/TSG.2012.2217991.

[12] Scrivener, K., Martirena, F., Bishnoi, S., & Maity, S. (2018). Calcined clay limestone cements (LC3). Cement and Concrete Research, 114, 49-56. https://doi.org/10.1016/j.cemconres.2017.08.017.

[13] Huld, T., Müller, R., & Gambardella, A. (2012). A new solar radiation database for estimating PV performance in Europe and Africa. Solar Energy, 86(6), 1803-1815. https://doi.org/10.1016/j.solener.2012.03.006.

[14] Kalogirou, Soteris A. Solar energy engineering: processes and systems. Academic press, 2013.

[15] National Aeronautics and Space Administration. NASA POWER | Prediction Of Worldwide Energy Resources 2020. https://power.larc.nasa.gov/.

[16] International Renewable Energy Agency. (2021). *Renewable Power Generation Costs in 2021*. https://www.irena.org/publications/2022/Jul/Renewable-Power-Generation-Costs-in-2021.

[17] Danish Energy Agency. (2022). Technology Data for Industrial Process Heat. https://ens.dk/en/our-services/projections-and-models/technology-data/technology-data-industrial-process-heat.

[18] European Environment Agency. (2023). Greenhouse gas emission intensity of electricity generation in Europe. https://www.eea.europa.eu/ims/greenhouse-gas-emission-intensity-of-1.

[19] Department for Energy Security and Net Zero (2023). International industrial energy prices. https://www.gov.uk/government/statistical-data-sets/international-industrial-energy-prices.

[20] ENTSO-E (2023). Transparency Platform. https://transparency.entsoe.eu/dashboard/show.

[21] Ong, S., Campbell, C., Denholm, P., Margolis, R., & Heath, G.. (2013). *Land-Use Requirements for Solar Power Plants in the United States*. United States. https://doi.org/10.2172/1086349.

[22] Denholm, P, Hand, M, Jackson, M, & Ong, S. (2009). *Land Use Requirements of Modern Wind Power Plants in the United States*. United States. https://doi.org/10.2172/964608.